

EXPERIMENTAL STUDY ON DETERIORATION CHARACTERISTICS OF PARTIALLY REPAIRED RC SLABS UNDER FREEZING-THAWING AND FATIGUE COMBINED ACTION

K. KAKUMA, S. OKADA, S. OMOTE & H. NISHI
Civil Engineering Research Institute for Cold Region, Japan
kakuma@ceri.go.jp

ABSTRACT

As to bridge RC slabs in cold and snowy regions, the reduction of effective thickness due to frost damage of upper concrete affects load carrying capacity and fatigue durability. In Japan, actually, subsidence with upper frost damage has occasionally happened in RC slabs principally constructed in the late 1950s and 1960s, and it is predicted that the occurrence drastically increases in the near future. Accordingly, from the viewpoint of preventative maintenance to extend life of RC slabs, it is necessary to develop an upper repair method for cold and snowy environment. This study experimentally investigated the influence of upper repair on fatigue behaviour of RC slabs under frozen environment by using the experimental installation which can alternately apply both wheel running load repetitions and freezing-thawing cycles. From the experimental results, it was indicated that upper repair effect might not be sufficiently obtained in cold and snowy regions when using low durable materials against frozen environment, although the temporal improvement of fatigue durability was observed during frozen.

1. INTRODUCTION

The degradation of RC slabs of highway bridges is principally caused by the repetition of wheel running load of heavy vehicles: fatigue loading. In addition to fatigue, in cold and snowy regions, the reduction of cover thickness caused by frost damage of upper concrete due to snow melt water penetrating into slabs accelerated the reduction of load carrying capacity of slabs and results in bringing the shorter fatigue life than expected [1].

The examples of RC slabs with frost damage of upper concrete in Hokkaido, Japan are shown in Photograph 1. Photograph 1(a) is the case that upper cover concrete separated into mortar and aggregate by frost damage. In this case, water remained on concrete slab in spite of not after rainfall and damage depth exceeded upper cover thickness down to



(a) Frost damage of cover concrete



(b) Subsidence of RC slab

Photograph 1 - Typical deterioration of RC slabs in Hokkaido

upper reinforcement. Furthermore in Photograph 1(b) showing the subsidence of slabs, concrete around the hole deteriorated and separated into mortar and aggregate similar to the case of Photograph 1(a). From the field investigation of highway bridges in Hokkaido [2], it was reported that such fatigue-frost damage combined deterioration has spread in whole Hokkaido.

In cold and snowy regions, hence, the adequate maintaining of upper concrete is especially important to extend the life of RC slabs. In order to do so, a comprehensive and systematic management method, including a damage inspection, a soundness evaluation and repair or reinforcement technique, must be developed.

From the above backgrounds, authors have studied on the establishment of preventative repair method for frost damaged RC slabs intending to apply to slabs with comparatively low deterioration degree. In previous studies, fatigue test using upper repaired RC slabs revealed that a repair method using PAE polymer cement mortar, acrylic resin mortar or epoxy resin mortar for repair material with water jet surface treatment could recover fatigue lives up to sound state before damaged under dry and air environment [3]. For the next stage of series of studies, the influence of upper repair on fatigue durability and damage modes of RC slabs is experimentally investigated under low temperature that minimum temperature reach -20 degrees. Incidentally, this study handles the state RC slabs are frozen, and the repetition of freezing-thawing action inducing material deterioration is not considered.

2. TEST SPECIMEN

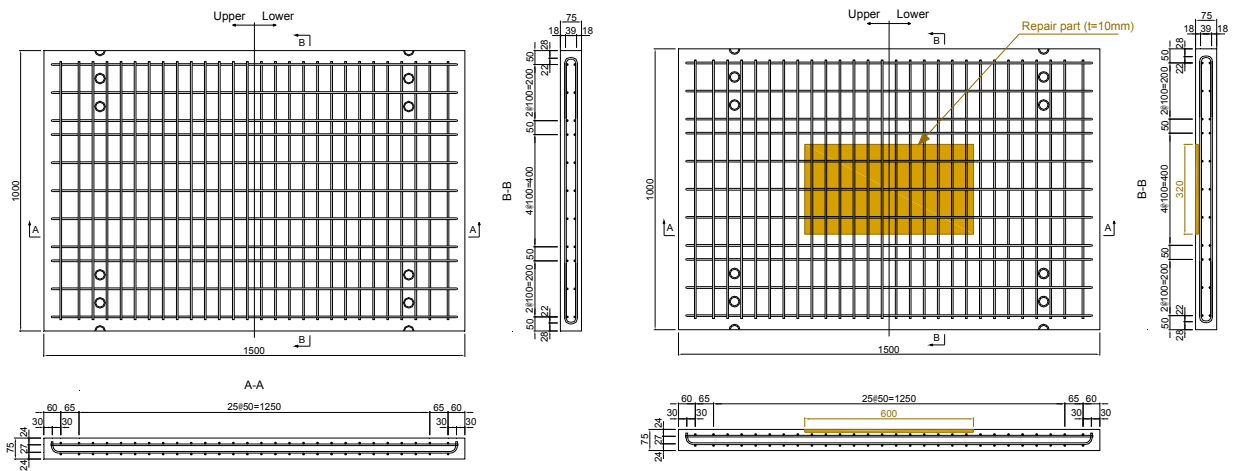
2.1. Outline of specimens

Three small-scale RC slab specimens with almost one-third dimension of actual road bridge slabs are prepared to evaluate the fatigue durability of RC slabs under cold environment. The specimens are designed in accordance with *the Specification for Highway Bridges* published by Japan Road Association in 1956 [4], because much deterioration have been reported from RC slabs constructed in the late 1950s and 1960s designed using the specification and many of highway bridges of the era are subjected to be repaired by Ministry of Land, Infrastructure, Transport and Tourism in Japan.

Table 1 lists the test specimens; Specimen-1 and Specimen-2 are non-repaired specimens tested under dry and frozen environment respectively, and Specimen-3 is upper-repaired specimen tested under frozen environment. Figure 1 shows the dimensions and the reinforcement arrangement of specimens. The specimens are 1,500mm long and 1,000mm long in longitudinal and transverse directions respectively with slab thickness of 75mm. Specimen-3 has a repair part with area of 600x340mm and thickness of 10mm in centre of specimen as shown in Figure 1(b). Repaired specimen is manufactured by (1)

Table 1 - List of test specimens

Specimen	Repair	Environment
Specimen-1	No	Dry
Specimen-2	No	Frozen
Specimen-3	Yes	Frozen



(a) Specimen-1 and Specimen-2

(b) Specimen-3

Figure 1 - Dimension and reinforcement arrangement of specimens

Table 2 - Mix proportion of slab concrete

Maximum aggregate size	W/C	Air content	Water	Cement	Sand	Coarse aggregate	Super plastisizer
mm	%	%	kg/m ³	kg/m ³	kg/m ³	kg/m ³	kg/m ³
10	48.8	4.5	159	326	923	931	3.26

Table 3 - Material properties

Specimen	No.1	No.2	No.3
Compressive strength of slab concrete (N/mm ²)	36.2	37.7	40.4
Young's modulus of slab concrete (kN/mm ²)	30.9	31.4	34.1
Compressive strength of repair concrete (N/mm ²)	-	-	50.2
Young's modulus of repair concrete (kN/mm ²)	-	-	27.2
Yield strength of reinforcement (N/mm ²)	337		
Young's modulus of reinforcement (kN/mm ²)	200*		

* design value

making a depression by water jet chipping and (2) backfilling the depression by repair material.

2.2. Materials

For slab concrete, ordinary Portland cement and coarse aggregate with maximum 10mm diameter are used. For both main and distribution reinforcements, round bar with 6mm diameter of SR235 is used. For upper repair part in Specimen-3, ultra rapid hardening mortar, which is often used for upper repair of RC slabs in Japan, is used. Table 2 and 3 show the mix proportion of slab concrete and the mechanical properties of concrete materials obtained from the cylinder tests.

3. TEST PROCEDURE

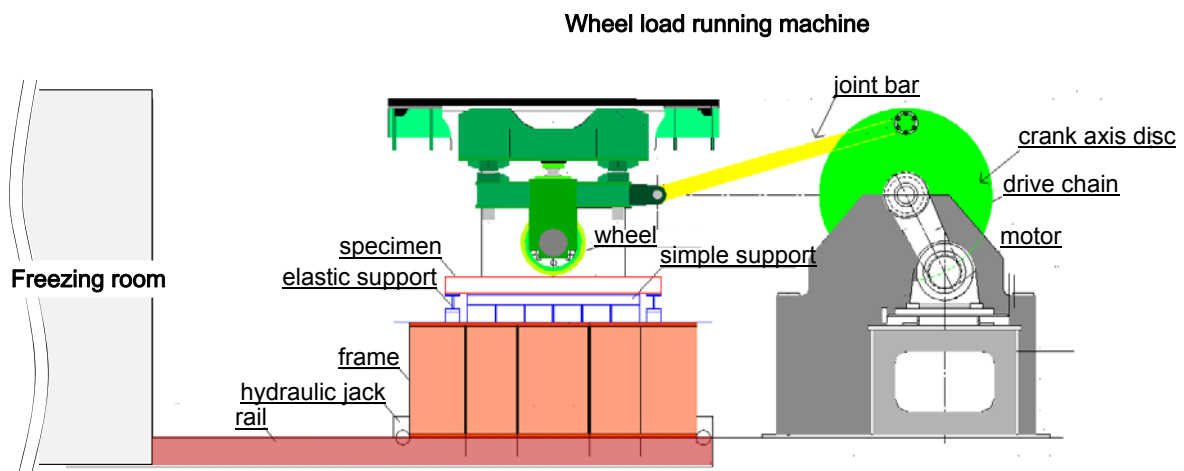
3.1. Experimental installation

For fatigue test, this study uses a loading installation which can alternately apply both wheel running load repetitions and freezing-thawing cycles on specimens; consists of a wheel load running machine for applying fatigue load, a freezing room for applying freezing-thawing action and a freezing device to keep specimen at low temperature as much as possible while running (shown in Figure 2(a)).

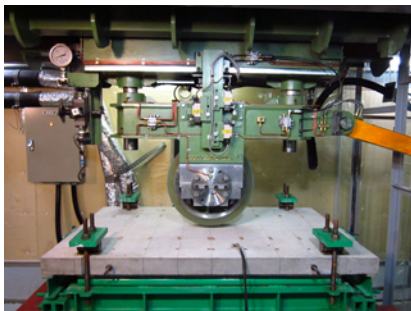
3.1.1 Wheel load running machine

The wheel load running machine is the quarter model of the machine originally developed by Matsui [5] to reproduce fatigue deterioration mechanism and evaluate durability of RC slabs (shown in Figure 2(b)). The specifications of the machine used in this study are shown in Table 4. It is a crank-driven machine and can continuously apply a maximum load of 40kN by hydraulics while running. Wheel can run in 1,000mm distance; 500mm back and 500mm forth from the midspan of specimen in longitudinal direction, with the speed of 24 round trips in a minute under 50Hz of power supply frequency. Wheel is made of urethane with the dimension of 480mm outer diameter and 170mm width.

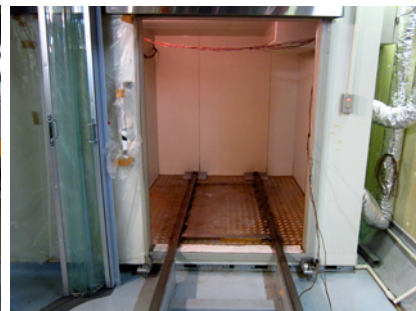
As shown in Figure 3, specimen is simply supported via round bar at the end of transverse direction corresponding to the support by main girder and elastically supported via H-shape steel girder with 100mm height and 50mm width at the end of longitudinal direction considering the continuity of RC slabs in actual road bridges. At four corners of specimen, anchor bolts are set to prevent a specimen from floating.



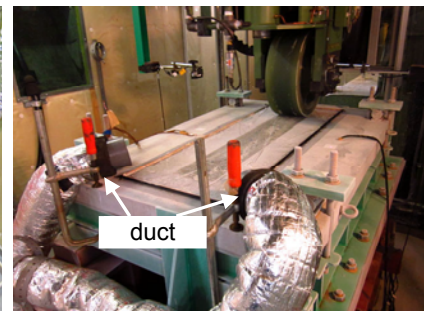
(a) Outline



(b) Wheel load running machine



(c) Freezing room

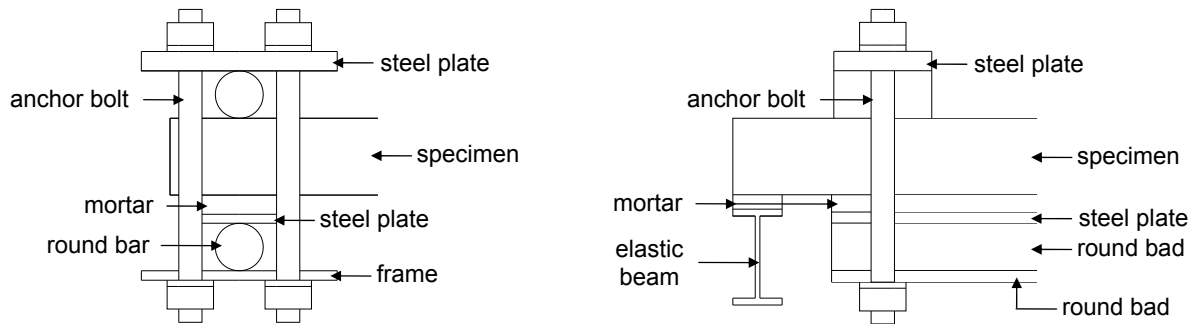


(d) Freezing device

Figure 2 - Experimental installation

Table 4 - Specifications of wheel load running machine

load	load	min.	10 kN
		max.	40 kN
	running range		1,000 mm
running speed		24 round trips/min (48 cycles/min)	
wheel	material		urethane
	outer diameter		480 mm
	width		170 mm



(a) Simple support (transverse direction) (b) Elastic support (longitudinal direction)

Figure 3 - Support condition

3.1.2 Freezing room

The freezing room of this experimental installation has the inside dimension of 1,190mm width, 1,670mm height and 2,000mm depth and can cool the inside temperature down to -20 degrees. Wheel load running machine is connected with the room by rails to move specimen with supporting frame manually (shown in Figure 2(c)).

3.1.3 Freezing device

The experimental installation is fabricated in a room with a constant temperature of 20 degrees. Accordingly, to keep specimen at low temperature, cold air in freezing room is sent to specimen via ducts and vinyl made curtains surround the loading machine during wheel load running (shown in Figure 2(d)).

3.2. Test program

Freezing action and wheel load running are reciprocally, not simultaneously, applied based on fixed manners. The manners are shown in the following.

3.2.1 Freezing

Specimens are frozen every 10,000 running cycles until total 80,000 running cycles and every 15,000 running cycles after total 80,000 running cycles in a state that a bank is built on top surface by caulking material and it is filled with water. Freezing minimum temperature is set to be -20 degrees, controlled by two thermocouples inserted in specimen. Incidentally, the temperature change during every 10,000 or 15,000 running cycles was -17 degrees minimum and 12 degrees maximum, and almost a half of whole wheel load running cycle was under frozen environment and another half was under melted environment.

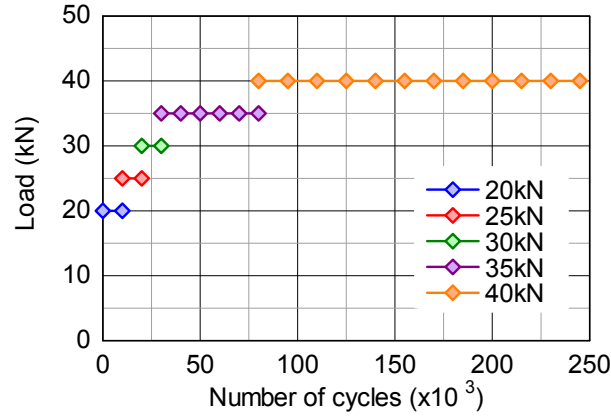


Figure 4 - Fatigue loading program

3.2.2 Fatigue loading program

The fatigue loading program is provided as shown in Figure 4. This test adopts a stepwise increase loading program increasing 5kN each at the specified number of cycles from 20kN to 40kN.

In the experiment, the bottom deflection of centre of specimen was measured by static loading of wheel load on the centre of specimen at the predetermined number of cycles. At the same time, crack distribution of both top and bottom surface of specimen are visually observed and debonding of cover concrete is investigated by hammering test.

3.3. Equivalent number of cycles

In this study, fatigue durability is evaluated by equivalent number of cycles assuming constant fatigue load, because the test adopts a stepwise increased loading program. Equivalent number of cycles is calculated from Equation 1 when fatigue deterioration of RC slabs depend on Miner's cumulative damage law.

$$N_{eq} = \sum \left(\frac{P_i}{P} \right)^m N_i \quad (1)$$

where,

- N_{eq} : Equivalent number of cycles
- P_i : Fatigue load (kN)
- P : Imposed load (kN)
- m : Reciprocal of the slope of S-N diagram
- n_i : Number of cycles under P_i

Here, imposed load, P , is set to be 30kN. Also, for the reciprocal of the slope of S-N diagram, m , 12.76 (=1/0.07835) is applied from the S-N diagram derived by Matsui [5].

$$\log \left(\frac{P}{P_{sx}} \right) = -0.07835 \log N + \log 1.52 \quad (2)$$

where,

- P : Fatigue load (kN)
- P_{sx} : Punching shear strength of the slab deteriorated into like multi-beams (kN)
- N : Number of cycles

Punching shear strength of the slab deteriorated into like multi-beams, P_{sx} , is calculated from the next equation.

$$P_{sx} = 2\tau_{smax} \cdot X_m \cdot B + 2\sigma_{tmax} \cdot C_m \cdot B \quad (3)$$

where,

- τ_{smax} : Maximum shear stress of concrete (N/mm²) = $0.65f'_{ck}{}^{0.606}$
- X_m : Neutral axis that ignores the tension zone concrete (mm)
- B : Beam width of the slabs deteriorated into like multi-beams (mm)
= $b+2d_d$
- b : Side length of the loading plate in the direction of the distribution reinforcement (mm)
- d_d : Effective height of the distribution reinforcement in the tension zone (mm)
- σ_{tmax} : Maximum tensile stress of concrete (N/mm²) = $0.269f'_{ck}{}^{2/3}$
- C_m : Thickness of cover concrete on the main reinforcement (mm)
- f'_{ck} : Concrete strength (N/mm²)

4. RESULTS AND DISCUSSIONS

4.1. Deflection

4.1.1 Specimen-1

The deflection-equivalent number of cycles relation of Specimen-1 is plotted by black dots in Figure 5.

As to Specimen-1, shear failure occurred at 75,373 running cycles with rapid increase of deflection after showing stepwise deflection change as the slope of deflection change increased gradually with the increase of fatigue load.

4.1.2 Specimen-2

The deflection-equivalent number of cycles relation of Specimen-2 is plotted by blue dots in Figure 5.

As to Specimen-2, deflection changed at almost half degree of Specimen-1 and it showed serrated characteristic behaviour during wheel load running. This was because apparent increase of slab stiffness, while inner temperature of specimen was kept under 0 degrees, prevented fatigue deterioration from developing. Figure 6, the relation between deflection, inner temperature and equivalent number of cycles until 100,000 running cycles, obviously revealed frozen state less than 0 degrees decreased deflection temporarily and the progress of fatigue deterioration resumed under melted state more than degrees.

Experiment finally finished at 183,565 running cycles with the developing of separation of mortar and aggregate in upper part of concrete, bringing the difficulty of wheel load running due to the unevenness surface. Although the specified sudden increase of deflection could not be observed, the envelope curve of deflection change, which showed the slope of deflection change considerably increased after 100,000 running cycles, suggested the specimen came up to just before failure. After final running, actually, deterioration index of deflection calculated from the following equation was 0.84 [5].

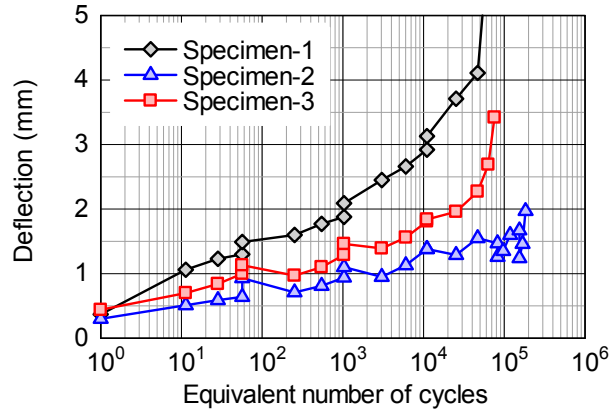


Figure 5 - Deflection-Equivalent number of cycles relation

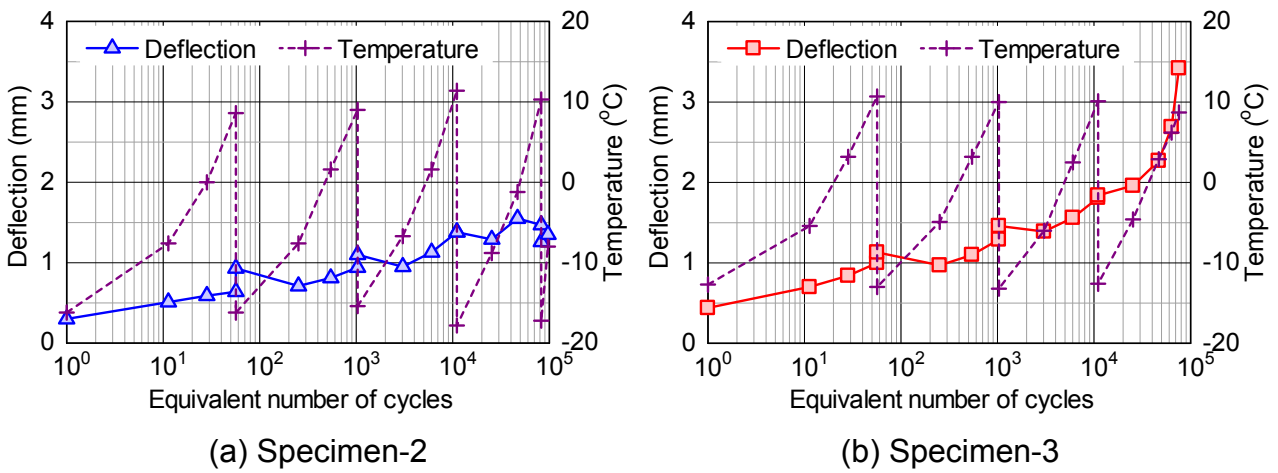


Figure 6 - Deflection-Inner temperature-Equivalent number of cycles relation

$$D_d = \frac{W - W_0}{W_c - W_0} \quad (4)$$

where,

- D/I : Deterioration index of deflection
- W : Experimentally measured deflection (mm)
- W_0 : Theoretical deflection calculated using total cross section (mm)
- W_c : Theoretical deflection calculated using RC cross section neglecting tensile concrete (mm)

4.1.3 Specimen-3

The deflection-equivalent number of cycles relation of Specimen-3 is plotted by red dots in Figure 5.

As to Specimen-3, fatigue failure occurred with rapid increase of deflection at 75,659 running cycles after the similar serrated deflection change to Specimen-2. Throughout experiment, deflection changed at approximately 1.3 to 1.5 times larger than Specimen-2, since repair material with relatively lower elastic modulus than slab concrete artificially behaved as cushioning, distributed load and brought the increase of crack density. Figure 7 shows the crack density-equivalent number of cycles relation. Here, crack density is

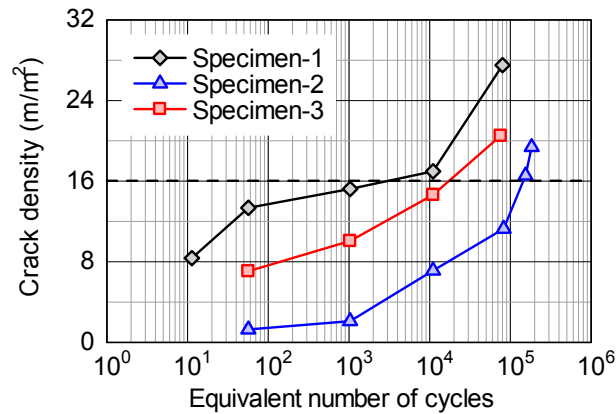


Figure 7 - Deflection-Equivalent number of cycles relation

defined as total crack length measured in the range of central 900x500mm in bottom surface of specimen. From Figure 7, it seems Specimen-3 obviously distributed cracks compared with Specimen-2 just after the start of wheel load running.

4.2. Failure condition

Figure 8 shows the failure condition of bottom and top surfaces of all specimens after experiment finished. In the figure, blue, red and green area show separation of aggregate from concrete, falling of upper cover concrete and debonding of upper cover concrete detected by hammering test, respectively.

4.2.1 Specimen-1

Failure condition of Specimen-1 was similar to a typical fatigue failure mode of RC slabs, i.e. hexagonal cracks initiated in bottom surface became dense and developed to cracks penetrating the slab from bottom to top, and finally punching shear failure occurred with falling down of bottom concrete where coloured by red in Figure 8(a). Upper cover concrete seemed to be peeled off from lower section just under wheel load running position after 11,033 running cycles and upper concrete was partially lost along running lane at failure. This was probably caused by abrasion between wheel and specimen and the difference damage type from circular or elliptical shape damage shown from fatigue loading under water environment.

4.2.2 Specimen-2

In Specimen-2, initial and midterm damage condition, meaning before the developing of hexagonal cracks and the penetrating toward height direction, were similar to Specimen-1. At 82,522 running cycles, the education of efflorescence was observed at both centre and one end of running lane in bottom surface. Also, debonding of upper cover concrete along wheel load running lane and separation of aggregate in upper concrete just over the position of efflorescence educating occurred at the almost same time, 154,012 running cycles. Finally, the aggregate separation depth in upper concrete deepened to 8mm at the end of experiment, 183,565 running cycles.

4.2.3 Specimen-3

In Specimen-3 showing different damage process from Specimen-2, partial aggregate separation of repair material initiated at 63,563 running cycles prior to efflorescence educating from bottom surface and debonding of upper cover concrete. This suggests ultra rapid hardening concrete, often used for upper repair of RC slabs in Japan, might have

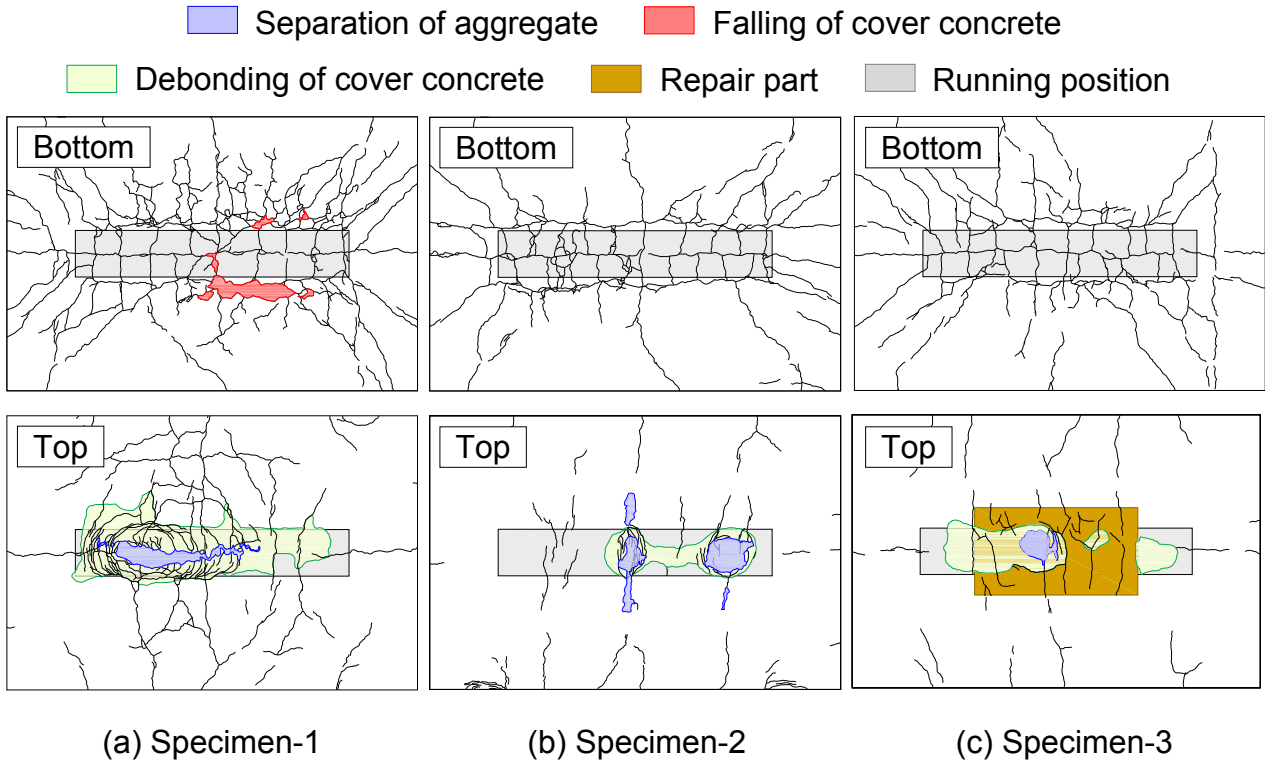


Figure 8 - Crack patterns in bottom and top surfaces

comparatively low durability compared with the structural durability of RC slabs and brings smaller repair effect in cold environment than in warm environment. Aggregate separation was finally 11.8mm depth reaching slab concrete at the position where damage was the most terrible, corresponding to the local reduction of slab thickness down to 85% of initial one. Based on the punching shear strength equation proposed by Masui [5], Equation 5, 15% of upper thickness reduction decreases punching shear strength down to 70% as to this test specimen. As mentioned below, actually, final failure was occurred at this most damaged position, and the reduction of load carrying capacity due to thus thickness reduction became the dominant factor of fatigue failure in Specimen-3.

$$P_0 = f_v [2(a + 2X_m)X_d + 2(b + 2X_d)X_m] + f_t [2(a + 2d_m)C_d + 2(b + 2d_d + 4C_d)C_m] \quad (5)$$

where,

- P_0 : Punching shear strength of RC slabs (kN)
- a, b : Length of loading plate for transverse and longitudinal direction (mm)
- X_m, X_d : Neutral axis depth for transverse and longitudinal cross section neglecting tensile concrete (mm)
- d_m, d_d : Effective height of lower main and distribution reinforcements (mm)
- C_m, C_d : Cover thickness of lower main and distribution reinforcements (mm)
- f_v : Shear strength of concrete (N/mm^2) = $0.656 f'_{ck}{}^{0.606}$
- f_t : Tensile strength of concrete (N/mm^2) = $0.269 f'_{ck}{}^{2/3}$
- f'_{ck} : Compressive strength of concrete (N/mm^2)

After experiment, for Specimen-3, cut cross section of specimen was observed in order to investigate damage condition, especially about debonding of repair material, in detail. Figure 9 shows the crack patterns of cross sections in transverse and longitudinal direction. From the observation of transverse cross section shown in Figure 9(a), it can be seen that

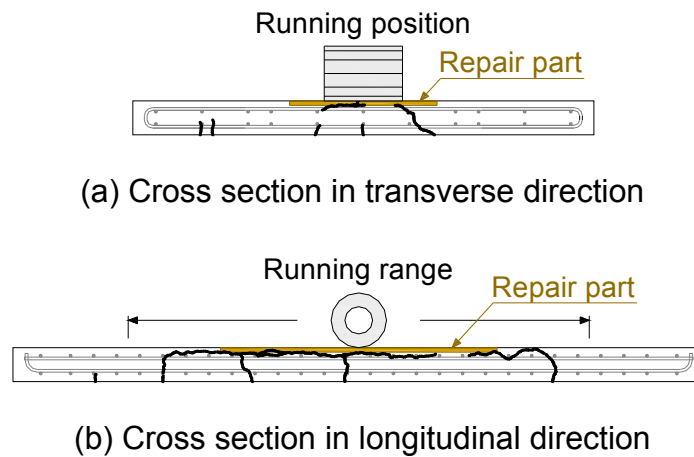


Figure 9 - Cross sectional crack pattern of Specimen-3

shear crack developed from the end of wheel loading position to bottom surface, indicating punching shear failure of slab concrete was the final failure mode of Specimen-3, while failure mode could not be determined from the surface crack pattern. This failure occurred at centre of specimen where aggregate separation of repair material also occurred. From longitudinal cross section shown in Figure 9(b), it seems that horizontal crack initiated in upper part of specimen along the whole wheel running range, including cracks appeared in both slab concrete and interface between slab concrete and repair material. Although a further investigation might be necessary to evaluate the structural integrity of repaired slabs, it seemed that the adhesion between repair material and slab concrete was sufficient to retain structural performance since no preceded interfacial separation of repair material and slab concrete was observed.

4.3. Evaluation of fatigue life

Figure 10 plots the fatigue lives of all specimens with SN diagram of RC slabs proposed by Matsui to clarify upper repair effect under frozen environment. About Specimen-2 before fractured, final equivalent number of cycles is regarded as fatigue life because the change of deflection and crack pattern indicated the symptoms of failure.

When comparing Specimen-1 and Specimen-2 to evaluate the effect of freezing, the fatigue durability of Specimen-2 was almost 2.5 times of Specimen-1. The experiment under frozen environment in this study allowed temperature to rise and wheel load running proceeded in the state that frozen state and melted state, it was almost the same meaning as in water environment, interchanged alternately. Although it has generally known that water environment shortens fatigue durability of RC slabs to 1/10 times or less of that under dry environment, the restraining effect of the increase in slab stiffness at below 0 degrees exceeded the decreasing effect of water.

As to Specimen-2 and Specimen-3, the fatigue life of upper repair specimen, Specimen-3, resulted in 1/2.5 times of non-repaired one, Specimen-2, under frozen environment. In Specimen-3, the decreasing effect of aggregate separation of repair material on fatigue durability was significant to cancel the fatigue life extension by freezing effect and the fatigue life was almost same degree as that of Specimen-1. Provided that, it is necessary to conduct additional wheel load running tests under perfect frozen environment refusing melted state and perfect or partial submerged environment in order to validate these effects.

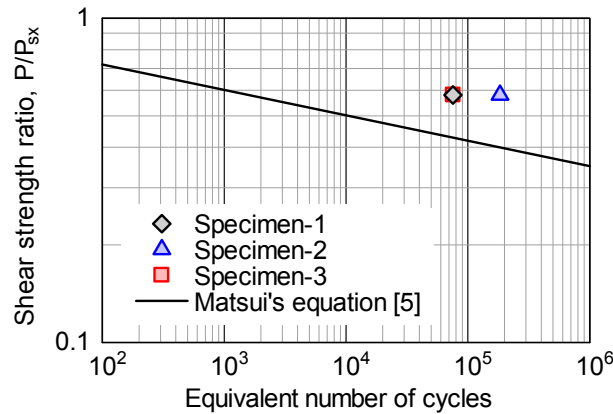


Figure 10 - Experimental fatigue lives and S-N diagram

5. CONCLUSIONS

Wheel load running tests of RC slab specimens were conducted to investigate the fatigue behaviour of frozen slabs and the influence of upper repair on fatigue durability under frozen environment. As the result, the followings were obtained.

1. Under frozen environment, apparent increase of slab stiffness while frozen at below 0 degrees improved fatigue durability and extended fatigue lives to 2.5 times of that under dry environment.
2. For upper repair in cold environment, the separation of aggregate and mortar of repair material bringing the reduction of effective slab thickness might shorten fatigue lives when using low durable materials against frozen environment.

This experiment was performed as one of series of studies intending to evaluate fatigue durability of RC slabs and establish suitable repair method for cold and snowy regions. To achieve the objectives, in the future studies, the influence of material deterioration due to frost damage, long-term freezing-thawing cycles, on fatigue durability should be evaluated and the development of the selection method of appropriate repair materials for cold and snowy regions.

REFERENCES

1. Ono T., Hayashikawa T., Mitamura H. and Matsui S. (2008). Study on Durability Improvement of Reinforced Concrete Slabs in Snowy Cold Region. Proceedings of 63rd JSCE Annual Meeting, pp 855-856 (in Japanese)
2. Mitamura H., Satou T., Honda K. and Matsui S. (2008). Influence of Frost Damage on Fatigue Failure of RC Deck Slabs on Road Bridges. Journal of Structural Engineering. Vol 55A, pp 1420-1431 (in Japanese)
3. Omote S., Mitamura H., Matsui S. and Hayashikawa T. (2012). Experimental Study on Fatigue Resistance of Frost-damaged Slabs after Partial Repair Work. Proceedings of 9th German-Japanese Bridge Symposium. paper 3C.6
4. Japan Road Association (1956). Specification For Highway Bridges (in Japanese)
5. Matsui S. (2007). Construction and Maintenance of Reinforced Concrete Deck Slabs on Highway Bridges. Morikita press (in Japanese)